

# CONTACT ANGLE HYSTERESIS EFFECTS ON THE RELATIVE PERMEABILITY OF GAS AND CONDENSATE IN THREE-DIMENSIONAL PORE NETWORKS

CECILIA I. BUSTOS and PEDRO G. TOLEDO

*Chemical Engineering Department and Surface Analysis Laboratory (ASIF), University of Concepción  
PO Box 160-C, Correo 3, Concepción, Chile  
[petoledo@udec.cl](mailto:petoledo@udec.cl)*

**Abstract -- The effect of contact angle hysteresis on the relative permeability of gas and condensate is studied with a mechanistic pore-level model of retrograde condensation in three dimensional pore networks under gravitational forces. We examine the effects of changing the wettability of the fluid-solid system from strongly liquid-wet to intermediate gas-wet.**

**Keywords -- capillary condensation, network modeling, relative permeability, contact angle hysteresis, wettability, Monte Carlo simulation**

## I. INTRODUCTION

A better understanding of phase distribution and flow in gas-condensate reservoirs is essential for optimum exploitation strategies. When pressure, either in the wellbore or in the reservoir, drops below the dew point a new phase appears, a phenomenon known as retrograde condensation. At first, the new condensate phase remains immobile blocking few gas paths; the gas effective permeability remains high. As the pressure decreases, condensate dropout tends to occupy more and more gas paths, attaining the so-called critical condensate saturation at which the liquid phase becomes mobile for the first time, and the gas effective permeability decreases. How abruptly it decreases depends on the pore structure, fluid properties and operating conditions. The critical condensate saturation and the relative permeability of gas and condensate are essential parameters for the evaluation and development of new designs of gas and condensate recovery strategies.

Literature reviews of laboratory studies of critical condensate saturation and relative permeability of gas and condensate are provided by Wang and Mohanty (1999), Blom *et al.* (2000), Jamiolahmady *et al.* (2000) and Li and Firoozabadi (2000).

Pore-level models of condensation dealing with the various aspects of the process have been developed by Mohammadi *et al.* (1990), Fang *et al.* (1996), Toledo and Firoozabadi (1998), Wang and Mohanty (1999), Li and Firoozabadi (2000) and Jamiolahmady *et al.* (2000). Recently we developed a mechanistic model of the retrograde condensation process in three-dimensional pore networks under gravitational forces (Bustos and Toledo, 2002a). In that work we reported new gas and

condensate relative permeabilities as a function of condensate saturation for various system and simulation parameters and conditions. In a companion work (Bustos and Toledo, 2002b), we used the model to study the sensitivity of relative permeability of gas and condensate to pore size distribution.

In this paper we use the condensation model to examine the effects of changing the wettability of the fluid-solid system on the distribution of gas and condensate and thus on their relative permeabilities. Wettability is changed from strongly to intermediate liquid-wet. Li and Firoozabadi (2000) first studied this aspect from a modeling point of view, although restricted to two-dimensional networks.

## II. NETWORK MODEL

A summary of the model is presented emphasizing key aspects for the work here. A three-dimensional cubic network of pore segments represents porous media. Nodes at which the pore segments are connected act only as volumeless junctions with infinite conductance. Pore segments are rectilinear with polygonal cross sections circumscribing circles with distributed radii. Pore segment radius  $r_i$  is randomly assigned according to a given probability density function. Condensate accumulation in pore corners allows for condensate connectivity throughout the network, no matter how high the pressure is. We allow for contact angle hysteresis, which is characterized by advancing,  $\theta_A$ , and receding,  $\theta_R$ , contact angles; the advancing contact angle being always greater than the receding contact angle. Contact angle hysteresis arises when the liquid-vapor interface is unable to retrace its original path when it recedes on a solid surface. Pore segment length  $l$  is constant and chosen to accommodate the highest stable condensate column in vertical pore segments without overflowing.

The volume of condensate residing in the corners of a pore segment of arbitrary polygonal cross section is given by the general formula (see Fig. 1),

$$V_c = n r_w^2 l \times \left[ \sin(\alpha + \theta) \cos(\alpha + \theta) + \frac{\cos^2(\alpha + \theta)}{\operatorname{tg} \alpha} - \frac{\pi}{2} + \alpha + \theta \right] \quad (1)$$

where  $V_c$  is the volume of condensate at the corners of a pore,  $n$  is the number of sides of the polygonal cross section of the pore,  $r_w$  is the radius of curvature of the longitudinal meniscus, defined as

$$r_w = \gamma / P_{\text{cap}} \quad (2)$$

where  $\gamma$  is the interfacial tension,  $P_{\text{cap}}$  is the capillary pressure defined as  $P_g - P_c$ , where  $P_g$  is the pressure in the gas phase and  $P_c$  in the condensate phase,  $l$  is the pore length,  $\alpha$  is the corner half angle, and  $\theta$  is the contact angle -which we assumed equal to the receding contact angle.

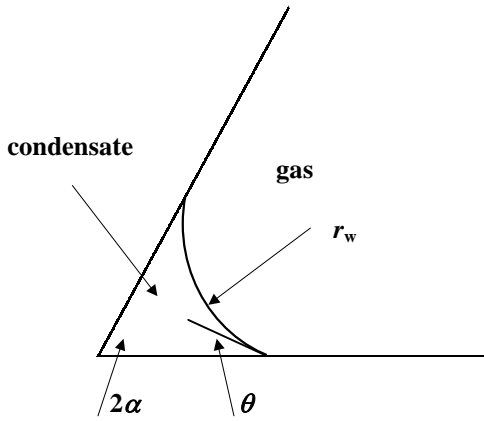


**Figure 1. Condensate wedge in a pore corner of semiapical angle  $\alpha$ .**

The capillary pressure that produces the bridge of condensate corresponds to the pressure at which the contact between the gas phase and the pore walls is lost. This configuration is highly unstable; an infinitesimal addition of condensate produces the snap-off of the gas-condensate interface and the formation of a bridge. The snap-off pressure  $P_s$  is given by (Lenormand, 1983)

$$P_s = P_g - P_c = \frac{\gamma \cos(\alpha + \theta)}{r_t \cos \alpha} \quad (3)$$

Again,  $\theta$  is the receding contact angle. The critical height of the condensate column for which the condensate begins to flow to the lower end of the pore segment can be calculated from (Fang *et al.*, 1996)

$$h_c = \frac{2\gamma}{\rho g r_t} (\cos \theta_R - \cos \theta_A) \quad (4)$$

where  $h_c$  is the condensate height and  $\rho$  is the condensate density (see Fig. 2). Condensate saturation is easily calculated from  $h_c$  and the shape of the pore segment.

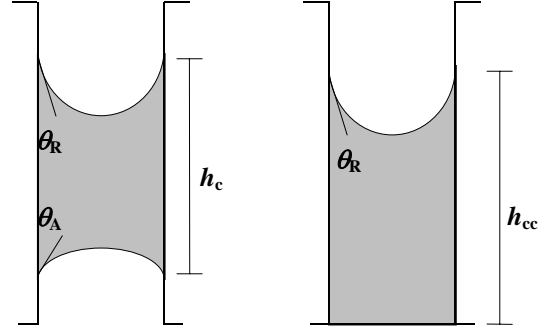


**Figure 2. Condensate bridge at the center and bottom of a pore segment.**

The critical condensate height inside a pore that produces dripping of condensate from the bottom can be calculated from (Fang *et al.*, 1996)

$$h_{cc} = \frac{2\gamma}{\rho g r_t} \cos \theta_R \quad (5)$$

where  $h_{cc}$  is the critical condensate height. In this case a flat meniscus is assumed at the bottom end of the pore segment.

From a simulation point of view, condensate dropout in a given vertical pore occurs by a cycling process, comprising: a) condensation until a capillary bridge is formed, b) additional condensation until the condensate column becomes unstable and dripping begins, c) brief reopening of the pore to the flow of gas, and d) formation of a new condensate bridge at the prevailing capillary pressure. This process repeats itself endlessly.

For horizontal pore segments, once the snap-off pressure is reached, further condensate dropout forms a bridge. The condensation process continues until the condensate fills the pore segment completely. Further condensate dropout drips from the ends of the pore segment. Condensate configurations in horizontal pore segments are not affected significantly by gravity.

From a simulation viewpoint, condensate dropout in horizontal pore segments occurs in two steps: condensation until the capillary bridge is formed, and further condensation until the condensate saturates the pore completely and condensate dripping begins. This last configuration is stable.

The continuous condensation process is discretized in steps, an idea first introduced by Fang *et al.* (1996). A small amount of condensate is added to each pore segment per step. Capillary equilibrium throughout the network is forced at the end of each step. As a consequence of adding condensate a pore may either increase its condensate inventory as wedges in pore corners if  $P_{\text{cap}} > P_s$  or form a bridge of condensate, or increase the length of a bridge if already exists, if  $P_{\text{cap}} \leq P_s$ .

Once the condensate phase reaches the percolation threshold of sample-spanning paths of condensate-filled

pore-segments, in the absence of a significant external pressure gradient, the gas flow stops. Then the gas effective permeability becomes zero.

A complex flow mechanism may arise for the gas phase. A gas island may be reconnected to the gas flow-carrying backbone if two or more pores holding condensate and acting as barriers to the gas flow get free of condensate in a given cycle. Then the gas island reconnects to the main gas flow contributing to its overall conductance, although just for an instant. This mechanism is also included in our simulation of the condensation process.

The last mechanism we consider occurs during the downflow of an unstable condensate bridge. For the gas phase this implies advancement of a gas column above the condensate and displacement of a gas column below the condensate. This event contributes to the overall gas permeability if the gas phase connects with the sample-spanning paths of gas-filled pore segments.

A modified form of the Poiseuille's law defines the fluid, gas or condensate, conductance  $g$  of each pore segment, i.e.,

$$q = g \Delta p \quad (6)$$

where  $q$  is the volumetric flow of fluid through the pore and  $\Delta p$  is the pressure drop across the pore.  $g$  depends on the configuration adopted by the fluid phases. For instance, when gas occupies the center of a pore and condensate its corners, the pore-level gas conductance is approximated here by Poiseuille's law for an effective gas cylinder, i.e.,

$$g = \frac{\pi r_{\text{eff}}^4}{8\mu l} \quad (7)$$

where  $\mu$  is the fluid viscosity and  $r_{\text{eff}}$  is given by (Blunt, 1997)  $r_{\text{eff}} = (r_t + r_v)/2$ , where  $r_t$  is the radius of the circle circumscribed by the sides of the polygonal pore and  $r_v$  is an equivalent volume radius given by  $\pi r_v^2 l = V_f$  with  $V_f$  corresponding to the volume of gas in the pore segment. For stable circular cylinders of gas of radius  $r_t$ ,  $r_{\text{eff}} = r_t$ . Conductances for various other configurations are provided by Bustos and Toledo (2002a).

For any given gas-condensate capillary pressure each phase develops its own flow network to which conductance can be assigned in much the same way as for monophasic flow.

To find the distribution of nodal pressures in each flow network once an external pressure gradient is imposed we use an iterative solution of the system of equations. With the nodal pressures of a given flow network in hand, the flow rate everywhere is calculated and the network conductance computed from

$$\bar{g}_j = \frac{Q_j}{(P_{\text{in}} - P_{\text{out}})} \quad (8)$$

where  $\bar{g}_j$  is the network fluid conductance of the  $j$  phase,  $Q_j$  is the total flow of phase  $j$  throughout the network and  $P_{\text{in}} - P_{\text{out}}$  is the pressure difference across the network.

The slow flow of a viscous fluid  $j$  in the presence of a second fluid in a porous medium is commonly assumed to be described also by Darcy's law,

$$Q_j = \frac{k_j}{\mu_j} A \left( \frac{\Delta P}{L} \right)_j \quad (9)$$

where  $\mu_j$  is the viscosity of fluid  $j$ ,  $(\Delta P/L)_j$  is the pressure gradient on fluid  $j$  in the direction of the main flow, and  $k_j$  is the effective permeability of fluid  $j$ . The relative permeability  $k_{rj}$  of phase  $j$  is thus

$$k_{rj} = Q_j / Q \text{ or } k_{rj} = \bar{g}_j / \bar{g} \quad (10)$$

where  $Q$  and  $\bar{g}$  are respectively the volumetric flow rate and the effective conductance when the phase flows through the pore network alone.

### III. RESULTS AND DISCUSSIONS

The results here are based on the following data. Condensate density is 800 kg/m<sup>3</sup> and gas-condensate interfacial tension is 0.001 dynes/cm. We use three-dimensional networks of 20×20×20 nodes, with 24,000 pore segments. Bustos and Toledo (2002a) found that this size is enough to minimize network size effects. Pore segments are rectilinear with square cross-sections,  $\alpha = \pi/4$ , circumscribing circles of given radii. To decorate the networks, pore sizes are drawn from the truncated log-normal distributions, depicted in Fig. 3; mean pore radius is constant and equal to 55  $\mu\text{m}$ , standard deviation varies from 8 to 50  $\mu\text{m}$  (see Table 1). The higher the standard deviation the higher the skewness, towards the smaller pores, of the distribution. Pore length is constant and equal to 300  $\mu\text{m}$ . Condensate is added in increments of 2,000  $\mu\text{m}^3$  per step until the flow of gas is stopped.

Relative permeability and saturation of both gas and condensate are evaluated at each step. Different receding contact angles are studied,  $\theta_R = 0, 10, \text{ and } 20^\circ$ , and  $\theta_R < \theta_A = 30^\circ$ . The fluid-solid system is strongly liquid-wet when  $\theta_R = 0^\circ$ , and increasingly intermediate liquid-wet as  $\theta_R$  increases from zero.

Figures 4-7 show calculated gas and condensate relative permeabilities. Results correspond to 95% confidence intervals around the mean of 3 realizations of each pore size distribution. Previously, we showed (Bustos and Toledo, 2002a and 2002b) that the relative permeability of the gas phase has the typical inverted s-shaped form and shows two distinct regimes. The same pattern is observed for the gas relative permeability in Figs. 4-7 for narrow and broad pore-size distributions and for varying contact angle hysteresis. In the first regime, for a condensate saturation less than 20%, the gas relative permeability decreases slowly and linearly with saturation; condensate exists mainly as liquid wedges in pore corners. In the second regime, for condensate saturations higher than 20%, as pore segments become saturated with condensate, the gas relative permeability decreases faster, abruptly in cases. Near the percolation threshold of sample-spanning paths of condensate-filled pore-segments, the gas relative permeability recovers its low decreasing pace, until its flow is stopped and its effective permeability becomes zero. The gas relative permeability near the percolation threshold for the gas phase is knee-shaped. How abruptly the gas relative permeability decreases during the second regime clearly depends on pore size distribution and contact angle hysteresis, for all other parameters fixed as Figs. 4-7 show. The skewer the pore-size distribution the narrower the condensate saturation range for the second regime.

According to Figs. 4-7, the first regime is very similar for all the pore-size distributions and contact angle hysteresis tested except that the skewer the distribution the faster the gas relative permeability decreases with condensate saturation. During this regime, contact angle hysteresis has no appreciable effect on the gas relative permeability, because at low saturations of the condensate phase most pore segments hold condensate wedges in corners, but remain open to the gas flow. Varying the contact angle modifies the shape of the gas-condensate menisci (see Fig. 1), but of course this is not enough to modify significantly the gas

paths. The same argument serves to explain why the condensate relative permeability curves shown in Figs. 4-7 are quantitatively very similar. Figures 4-7 shows that during the first regime, the gas and condensate relative permeabilities display no significant sensitivity to changes in contact angle hysteresis.

In the second regime, Figs. 4-7 show that at any given saturation, the narrower the pore size distribution the higher the relative permeability of the gas phase, an effect already discussed in Bustos and Toledo (2002b). Pore networks decorated with wider and skewer pore-size distributions attain condensate saturations with a higher fraction of small pore segments saturated with condensate as compared to narrower distributions. Thus, for a given condensate saturation the gas relative permeability is lower for the network with wider and skewer distributions of pore sizes.

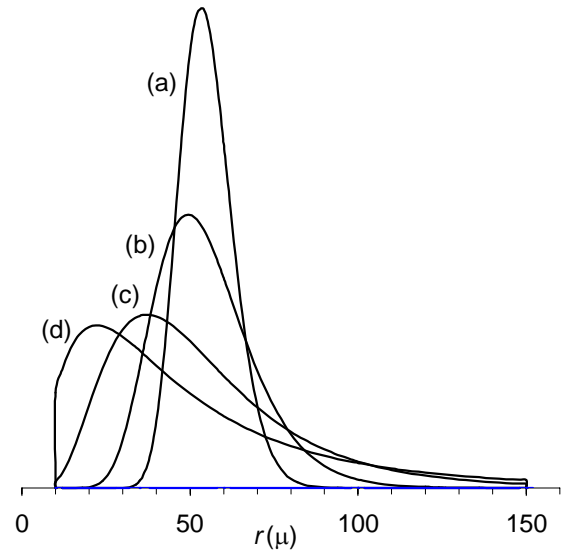


**Figure 3. Truncated log-normal pore size distributions. Parameters are listed in Table 1.**

**Table 1. Parent pore size distributions and parameters. Figure 3 shows graphical representations. A and B are adjustable constants.**

Log-normal distribution function $f(r_t)$	Parameters		
$\frac{1}{Br_t\sqrt{2\pi}} \exp\left[-\frac{1}{2}\left(\frac{\ln(r_t) - A}{B}\right)^2\right]$ $\mu = \exp\left[A + \frac{B^2}{2}\right]; \sigma^2 = \exp(2A + B^2) (\exp(B^2) - 1)$	$\mu = 55 \mu\text{m}$	$\sigma = 8 \mu\text{m}$	Fig. 3a
		$\sigma = 15 \mu\text{m}$	Fig. 3b
		$\sigma = 30 \mu\text{m}$	Fig. 3c
		$\sigma = 50 \mu\text{m}$	Fig. 3d

$r_{t,\min}$  = minimum pore radius;  $r_{t,\max}$  = maximum pore radius;  $\mu$  = mean pore radius;  $\sigma$  = standard deviation

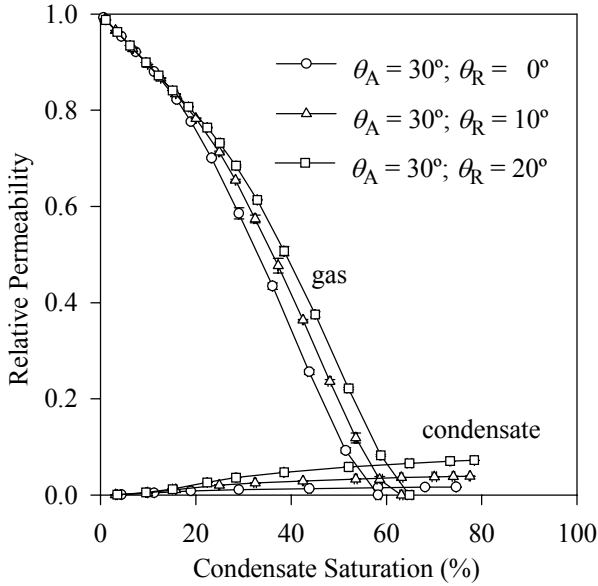


Figure 4. Gas and condensate relative permeabilities. Log-Normal distribution;  $\mu = 55 \mu\text{m}$ ;  $\sigma = 8 \mu\text{m}$ .

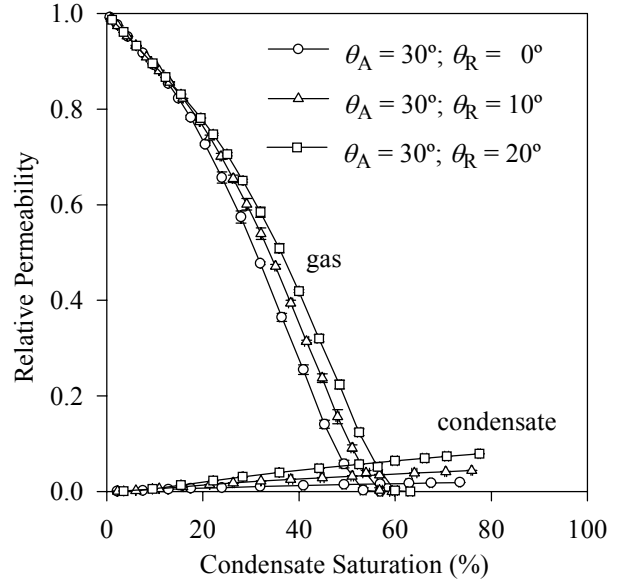


Figure 5. Gas and condensate relative permeabilities. Log-Normal distribution;  $\mu = 55 \mu\text{m}$ ;  $\sigma = 15 \mu\text{m}$ .

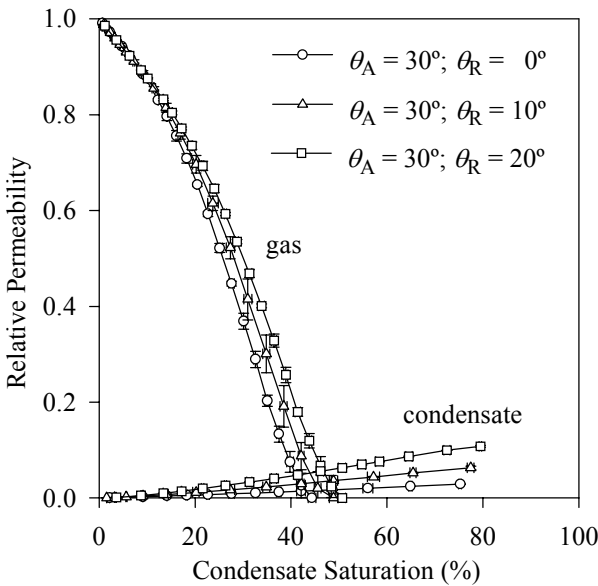


Figure 6. Gas and condensate relative permeabilities. Log-Normal distribution;  $\mu = 55 \mu\text{m}$ ;  $\sigma = 30 \mu\text{m}$ .

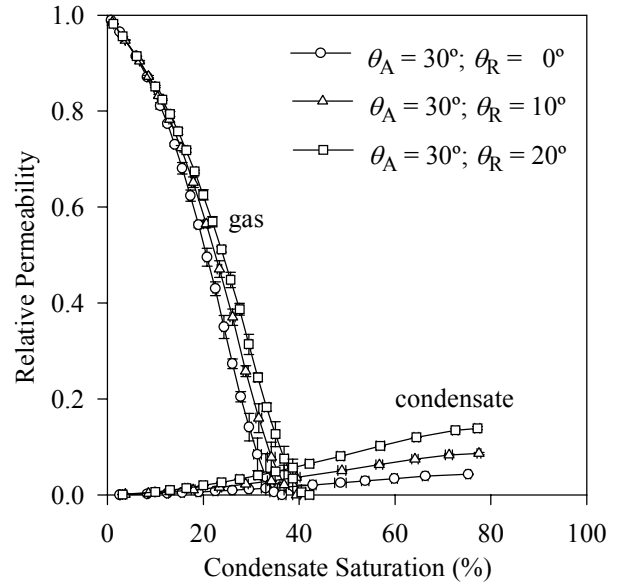


Figure 7. Gas and condensate relative permeabilities. Log-Normal distribution;  $\mu = 55 \mu\text{m}$ ;  $\sigma = 50 \mu\text{m}$ .

Figures 4-7 also show that in the second regime the relative permeability of the condensate phase barely increases as the pore size distribution becomes narrower. In all cases of size skewness, the smaller pore segments, available in large numbers, control the conductance of the condensate network. Large pore segments saturated with condensate, if exist, act merely as connectors of condensate but do not control the overall condensate conductance.

On a different ground, the effect of contact angle hysteresis is significant on both the gas and condensate

relative permeabilities in the second regime. Figures 4-7, for a given pore size distribution, show that the relative permeabilities of gas and condensate increase when the contact angle hysteresis decreases. Actually, both permeabilities increase when the receding contact angle increases, i.e., when the solid surface becomes less liquid-wet.

We found that the relative permeabilities of gas and condensate are not affected by the magnitude of the advancing contact angle. Li and Firoozabadi (2000) presented similar results regarding the effect of contact

angle hysteresis, except that they found a more pronounced effect than the one observed here. The explanation may well be the lower dimensionality of the networks used by these authors. According to the gas relative permeability obtained here for the second regime, we argue, as Li and Firoozabadi (2000) did, that gas well deliverability may increase significantly if the wettability of the near-well formation is kept more gas-wet than liquid-wet.

Near the percolation threshold for the gas phase, few remaining gas paths become blocked by condensate; the result is a slowly decaying gas relative permeability. At the end of the second regime, the flow of gas is stopped and its relative permeability becomes zero.

It should be noticed in Figs. 4-7 that for any given pore size distribution and after the flow of gas is stopped, condensate dropout continues until every horizontal pore segment becomes saturated. In this case, condensate relative permeability increases notably as the receding contact angle increases.

#### IV. CONCLUSIONS

A mechanistic model of the retrograde condensation process in three-dimensional pore networks under gravitational forces is used to determine the effect of contact angle hysteresis on the relative permeability of gas and condensate phases. Condensate wedges contribute to both condensate saturation and overall conductance.

The relative permeability of the gas phase shows two distinct regimes. In the first regime, the gas relative permeability decreases slowly at low saturations of condensate, while condensate exists mainly as liquid wedges in pore corners. In the second regime, as pore segments become fully saturated with condensate, the gas relative permeability decreases faster, abruptly in cases.

Regarding the effect of contact angle hysteresis during the first regime, the gas and condensate relative permeabilities display no significant sensitivity to changes in contact angle hysteresis.

Results for the second regime show that the relative permeabilities of gas and condensate increase significantly when the contact angle hysteresis decreases. Actually, both permeabilities increase when the receding contact angle increases, i.e., when the solid surface becomes less liquid-wet. We found that the relative permeabilities of gas and condensate are not affected by the magnitude of the advancing contact angle. According to the gas relative permeability obtained here for the second regime, we argue that gas well deliverability may increase significantly if the wettability of the near-well formation is kept more gas-wet than liquid-wet, a conclusion already advanced in the literature for two-dimensional pore networks.

#### ACKNOWLEDGEMENTS

We thank CONICYT of Chile for financial support through projects FONDECYT No. 2990056 and 1980462.

#### REFERENCES

- Blom, S. M. P., J. Hagoort and D. P. N. Soetekouw, "Relative Permeability at Near-Critical Conditions", *SPE Journal*, **5**(2), 172-181 (2000).
- Bustos, C. and P. G. Toledo. "Pore-Level Modeling of Gas and Condensate Flow in Two and Three Dimensional Pore Networks", Paper submitted to *Transport in Porous Media* (2002a).
- Bustos, C. and P. G. Toledo. "Pore Size Distribution and Pore Shape Effects on the Relative Permeability of Gas and Condensate in Three-Dimensional Pore Networks", Paper submitted to *Transport in Porous Media* (2002b).
- Blunt, M., "Effects of Heterogeneity and Wetting on Relative Permeability Using Pore Level Modeling", *SPE Journal*, **2**, 70-87 (1997).
- Fang, F., A. Firoozabadi, M. Abbaszadeh and C. Radke, "A Phenomenological Network Model of Critical Condensate Saturation", Paper SPE 36716 presented at the 1996 Annual Technical Conference and Exhibition held in Denver, Colorado, USA, 6-9 October (1996).
- Hughes, R. G. and M. J. Blunt, "Pore Scale Modeling of Rate Effects in Imbibition", *Transport in Porous Media*, **40** (3), 295-322 (2000).
- Jamiolahmady, M., A. Danesh, D. H. Tehrani and D. B. Duncan, "A Mechanistic Model of Gas-Condensate Flow in Pores", *Transport in Porous Media*, **41** (1), 17-46 (2000).
- Lenormand, R., C. Zarcane and A. Sarr, "Mechanisms of the Displacement of One Fluid by Another in a Network of Capillary Ducts", *J. Fluid. Mech.*, **135**, 337-353 (1983).
- Li, K. and A. Firoozabadi, "Phenomenological Modeling of Critical Condensate Saturation and Relative Permeabilities in Gas/Condensate Systems", *SPE Journal*, **5**(2), 138-147 (2000).
- Mohammadi, S., K. S. Sorbie, A. Danesh and J. M. Peden, "Pore-Level Modelling of Gas-Condensate Flow Through Horizontal Porous Media", Paper SPE 20479 presented at the 65<sup>th</sup> Annual Technical Conference and Exhibition of the Society of Petroleum Engineers held in New Orleans, LA, September 23-26 (1990).
- Toledo, P. G. and A. Firoozabadi, "Renormalization Calculations of Gas Relative Permeability in a Pore-Network of Gas-Condensate Systems", Paper SPE 39980 available through SPE (1998).
- Wang, X. and K. K. Mohanty, "Critical Condensate Saturation in Porous Media", *Journal of Colloid and Interface Science*, **214**, 416-426 (1999).